



RESEARCH ARTICLE

IMPACT OF QUENCHING ON STRUCTURAL AND MAGNETIC PROPERTIES OF
 $\text{Ni}_{0.5-x}\text{Zn}_x\text{Cu}_{0.5}\text{Fe}_2\text{O}_4$ MIXED FERRITES PREPARED USING SOLID STATE ROUTE

^{1,*}Senthilkumar, S., ¹Selvakumar, C., ¹Aravazhi, S., ²Chandrasekaran, G. and ³Sagayaraj, R.

¹PG and Research Department of Physics, Arignar Anna Govt Arts College Villupuram-605602, Tamilnadu, India

²Department of Physics, Pondicherry University, Pondicherry-605014, India

³PG and Research Department of Physics, St. Joseph's College of Arts & Science (Autonomous),
Cuddalore, 607001, Tamilnadu, India

ARTICLE INFO

Article History:

Received 21st October, 2017
Received in revised form
10th November, 2017
Accepted 28th December, 2017
Published online 31st January, 2018

Key words:

X-ray diffraction,
Thermal, FTIR,
Raman Spectroscopy,
Magnetic Measurement.

ABSTRACT

A system of Ferrites with formula $\text{Ni}_{0.5-x}\text{Zn}_x\text{Cu}_{0.5}\text{Fe}_2\text{O}_4$ ($x=0.0, 0.1, 0.2, 0.3, 0.4, 0.5$) synthesized through solid state route. During the second sintering the material is quenched from 1137 K to 77 K by dropping it in liquid nitrogen bath. The solid material is ground in agate pestle, mortar and made as powder. The powder form of ferrite is subjected to structural studies using XRD, thermal, FTIR and Raman measurements. XRD patterns present that the crystals formed are in the polycrystalline nature. The structure of ferrite is confirmed as Face Centred Cubic (FCC) phase. The particle size of the ferrite system varies from 262 to 427 Å and they are bulk particles. Thermal study helps to infer completion of reaction of formation of ferrite. FTIR and Raman spectroscopy measurements confirm the presence of tetrahedral and octahedral coordination of atoms in spinel structure of ferrite. However a dominating impact of defect states intruded in the structure of ferrite is visualized through FTIR and Raman spectra. The presence of defect states is attributed to mainly to the quenching of the ferrite by a large range of temperature. The existence of defect states will contribute a big variation in electrical and the magnetic properties.

Copyright © 2018, Senthilkumar et al. This is an open access article distributed under the Creative Commons Attribution License, which permits unrestricted use, distribution, and reproduction in any medium, provided the original work is properly cited.

Citation: Senthilkumar, S., Selvakumar, C., Aravazhi, S., Chandrasekaran, G. and Sagayaraj, R., 2018. "Impact of quenching on structural and magnetic properties of $\text{Ni}_{0.5-x}\text{Zn}_x\text{Cu}_{0.5}\text{Fe}_2\text{O}_4$ mixed ferrites prepared using solid state route", *International Journal of Current Research*, 10, (01), 64397-64402.

INTRODUCTION

Ferrites are candidate substances which find wide applications in microwavedevices, computer memories and magnetic recording (Özgür et al., 2009; Goldman, 2006). In view of their importance several researchers have studied the thermal and magnetic properties of ferrite materials in the past several years (Tatarchuk et al., 2017; Golkhatmi et al., 2017). Smit and Wijn (Smit, 1959) have systematically and elaborately studied the thermal (Kwon et al., 2017) and magnetic properties of the ferrites NiFe_2O_4 and CuFe_2O_4 . They have reported that the saturation magnetization value of NiFe_2O_4 is 300 Gauss at 0K and its Curie temperature is 585°C. For the CuFe_2O_4 the values are 160 Gauss 455°C respectively. Similarly Arrot and Goldman (Goldman, 2006) and Hartmann-Boutron and Imbert (Hartmann, 1968) have studied ZnFe_2O_4 magnetically and have found out ZnFe_2O_4 is antiferromagnetic below 263 K. Many attempts have been made to lower the Curie temperature of NiFe_2O_4 and CuFe_2O_4 and for increasing the transition point of ZnFe_2O_4 there by suitably tailoring the saturation magnetization resistivity, chemical stability and

mechanical hardness. Such attempts have been made possible by mixing the end member ferrites namely NiFe_2O_4 and CuFe_2O_4 (Golkhatmi et al., 2017), NiFe_2O_4 and ZnFe_2O_4 and ZnFe_2O_4 and CuFe_2O_4 (20-23). Continuing on the same lines, several reports of earlier researchers (Yue, 1999; Naghib et al., 2016; Gawas et al., 2016) on mixed ferrite of Ni-Zn-Cu have motivated to prepare ferrites of ternary mixtures to provide additional thermal and magnetic data. It's of interest to dope Zn^{2+} ions in some of sites of Ni^{2+} ions in Ni-Cu mixed ferrite system. It is known that the magnetic behaviour of Ni-Cu ferrite largely governed by Fe-O-Fe interaction and Ni-O-Fe interaction. Introducing Zn^{2+} ions in the spinel lattice is expected to bring in a substantial change in magnetization and Curie temperature and hence the properties (Erdemi, 2015). It's also of interest to investigate structural and magnetic properties of ferrites depending upon a) the different super exchange interaction developed in the ferrite and b) the effect caused by the cooling rate employed during the synthesis of the sample.

Experimental details

Synthesis

A series of ferrites with composition $\text{Ni}_{0.5-x}\text{Zn}_x\text{Cu}_{0.5}\text{Fe}_2\text{O}_4$ with $x = 0.0, 0.1, 0.2, 0.3, 0.4,$ and 0.5 are synthesized using

*Corresponding author: Senthilkumar, S.,

PG and Research Department of Physics, Arignar Anna Govt Arts College Villupuram-605602, Tamilnadu, India.

ceramic sintering procedure. All the reactants used are of AR grade NiO, ZnO, CuO, and Fe_2O_3 . The systematic procedure of preparation is highlighted in the flow chart given below. The reactant oxides are thoroughly mixed and grind well using in a pure platform of agate pestle and mortar yielding uniform and tiny powder particles. The powder is transferred to silica crucible and heated to 1137K by placing it in a muffle furnace with air atmosphere. It is maintained for 20 hrs and later gradually cooled to room temperature in steps of 100°C per hr. The burnt stuff is broken and crushed to form powder in a clean manner. The powder is made as pellet. The pellet is re-sintered at 1137 K. After this second sintering the pellet is quenched from 1137 K to 77 K by dropping it in liquid nitrogen bath. The solid material is ground in agate pestle, mortar and made as powder. The powder form of ferrite is subjected to structural studies using XRD, thermal, FTIR and Raman measurements.

Characterization

The XRD spectra of $\text{Ni}_{0.5-x}\text{Zn}_x\text{Cu}_{0.5}\text{Fe}_2\text{O}_4$ with $x = 0.0, 0.1, 0.2, 0.3, 0.4,$ and 0.5 are recorded using the PAN alytical X-ray Diffractometer (Model: X'Pert PRO) with an X-ray radiation source of $\text{Cu-K}\alpha$ ($\lambda_{\text{K}\alpha 1} = 1.54056 \text{ \AA}$; $\lambda_{\text{K}\alpha 2} = 1.54439 \text{ \AA}$). The thermal decomposition process of $\text{Ni}_{0.5-x}\text{Zn}_x\text{Cu}_{0.5}\text{Fe}_2\text{O}_4$ powders have been carried out using TG-DTA analysis (Make: TA instruments, Model: Q600 SDT). The FTIR spectra are observed using the SHIMADZU 8700 FTIR spectrometer at room temperature over the range 4000-350 cm^{-1} . Raman scattering spectra are recorded using Confocal micro-Raman spectrometer (Renishawin Via Reflex) having a liquid-nitrogen cooled charge-coupled device multichannel detector (256 pixels X 1024 pixels). The measurements are carried out with an excitation wavelength of 418 nm at room temperature. The acquisition time and illumination power of the laser used for the present study are 20 s and 1mw respectively. Magnetization $M(H)$ measurement were done using a vibrating sample magnetometer (VSM) Lakshore UK.

RESULTS AND DISCUSSION

X-Ray diffraction study

Fig1. Shows a typical XRD pattern of $\text{Ni}_{0.5-x}\text{Zn}_x\text{Cu}_{0.5}\text{Fe}_2\text{O}_4$ samples sintered at 1100°C. The pattern shows well resolved peaks indicating that the prepared $\text{Ni}_{0.5-x}\text{Zn}_x\text{Cu}_{0.5}\text{Fe}_2\text{O}_4$ ferrites are polycrystalline. They are characteristic peaks of a spinel structure which confirm the phase formation indicating absence of other impurity phases. All the peaks perfectly match with the crystalline phase of Face Centre Cubic structure of $\text{Ni}_{0.5-x}\text{Zn}_x\text{Cu}_{0.5}\text{Fe}_2\text{O}_4$ ferrite (JCPD card: 74-2082). Experimental determination of lattice constants, molecular density, particle size and porosity is done and they are given value of Table1. In the present system of ferrites, Cu^{2+} , Ni^{2+} , Zn^{2+} and Fe^{2+} are the constituent cations. Using knowledge of site preference of the ions and the ionic size data of the respective ions as in Table2. Substitution of the ions in A and B sites of spine structure will be elucidated along with lattice parameter. It is seen from Table1. that the lattice constant decreases with Zn enhancement. By comparing the ionic radii of Ni and Zn ions it can be said that it is not a direct replacement of Ni by Zn. It is so because ionic size of Ni^{2+} is smaller than Zn^{2+} which is contradicted by change in lattice constant values.

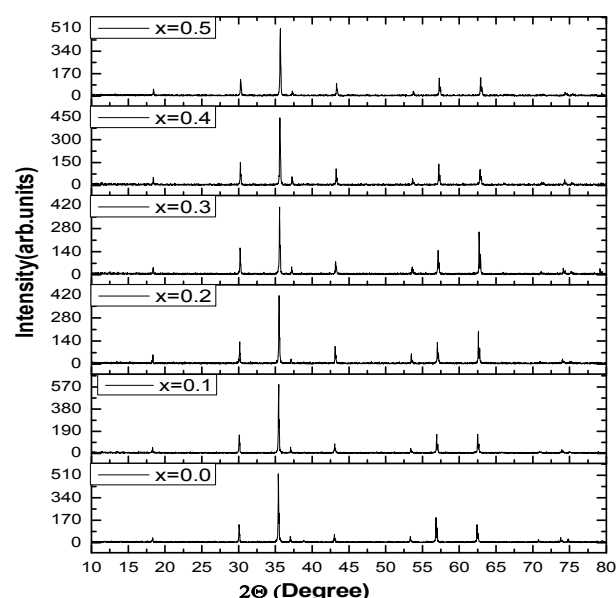


Figure 1. XRD patterns of $\text{Ni}_{0.5-x}\text{Zn}_x\text{Cu}_{0.5}\text{Fe}_2\text{O}_4$ system

It might be assigned to effect of migration of ions mutually between sites and ultrafine fine crystallite size. The crystallite size was calculated using Scherer's formula

$$D = 0.9\lambda / \beta \cos\theta$$

where, λ is the X-ray wavelength, β is the width of the peak and θ is the Bragg's position of the peaks (Murugesan *et al.*, 2014). The values of crystallite size are in the range from 262 to 427 \AA which is agreement with those reported by Parvatheeswararao *et al.* (1955). Molecular density rises with Zn substitution.

Thermal study

The phase transition points and phase formation are obtained by an analysis done using thermal data in STAR software for powder sample. The sample is taken in alumina crucible and heated and cooled in set temperature range between 100 and 900°C in steps of 20 °C/min. The specific heat curves of Ni-Zn-Cu mixed ferrites are plotted. The variation of specific heat flow with temperature for different concentration is shown in Fig. 2. The nature of the curves for specific heat of these ferrite samples certifies the completion of the chemical reaction meant for the preparation of ferrites. A shallow region of specific heat is a common trend observable around the phase transition point of these ferrites. It's expected that there is a phase transition around 550 – 570°C indicative of ferrimagnetic to paramagnetic phase (Viswanathan, 1990).

FT-IR Spectral Study

In order to confirm the formation of the spinel phase the FTIR spectra of the powders were recorded and shown in Fig 3. The spectra show characteristic absorption of ferrite phase. The strong absorption around 600 cm^{-1} and weak absorption in the range 480 cm^{-1} would correspond to tetrahedral and octahedral coordination ions respectively (Murugesan, 2015). This difference in the band position is expected because of difference in the system. $\text{Ni}_{0.5-x}\text{Zn}_x\text{Cu}_{0.5}\text{Fe}_2\text{O}_4$ ferrites for the octahedral and tetrahedral compounds. Waldron studied (Waldron, 1955) the vibrational spectra of ferrites and attributed the sharp absorption band around 600 cm^{-1} to the intrinsic vibrations of the tetrahedral group and 450 cm^{-1} to the other band of the octahedral group.

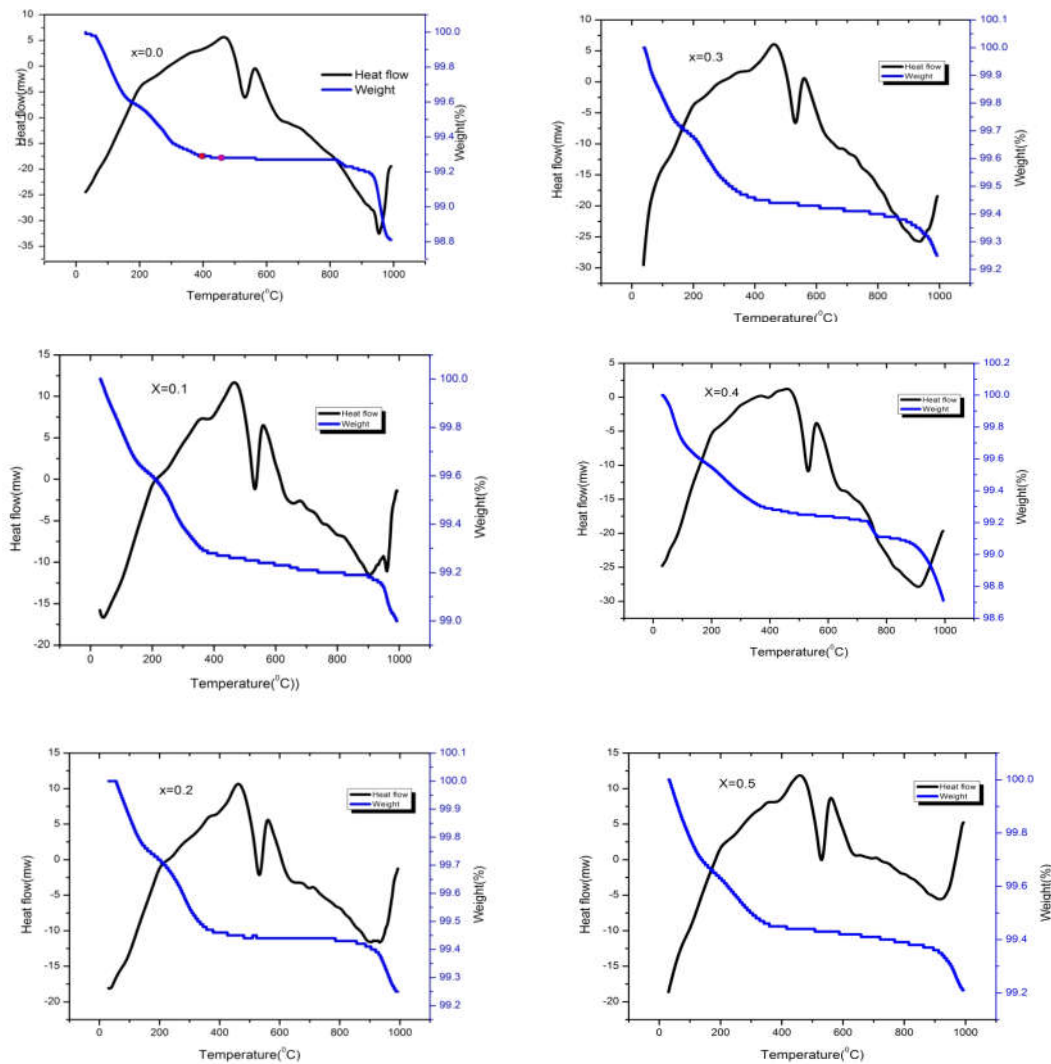


Figure 2. Thermographs of $\text{Ni}_{0.5-x}\text{Zn}_x\text{Cu}_{0.5}\text{Fe}_2\text{O}_4$ system

Table 1. Experimental lattice constants, particle size, porosity and molecular density of sintered $\text{Ni}_{0.5-x}\text{Zn}_x\text{Cu}_{0.5}\text{Fe}_2\text{O}_4$ ferrite system

Concentration (X)	lattice constant a (Å)	Crystallite Size (Å)	Molecular density ρ_m (Kg/m ³)	Porosity P%
0.0	8.4047	407.7735	5.2977	23.49
0.1	8.3941	427.4872	5.3328	29.45
0.2	8.3812	338.1855	5.3725	22.06
0.3	8.3669	275.7480	5.4153	27.26
0.4	8.3555	303.3100	5.4527	23.85
0.5	8.3429	262.7700	5.4927	24.87

It is clearly noticed from the spectra and Table 3. that the ferrites invariably contain octahedral and tetrahedral coordination of ions which are basic composite substructures of spinel. The shift of the bands indicative of encroachment of different ions in the sites when Zn is substituted. Further a higher value band around 650-800 cm^{-1} and above should indicate the formation of certain defect states in ferrites (Tarte, 1967; Chandrasekaran, 2000). It is bound to occur as the post sintering process is quenching. Normally quenching may lead to amorphous or defects state formation.

Raman Spectral Study

The room temperature Raman spectra of $\text{Ni}_{0.5-x}\text{Zn}_x\text{Cu}_{0.5}\text{Fe}_2\text{O}_4$ is observed in the range of 50-1000 cm^{-1} .

The observed vibrational modes are shown in Fig 4. They are found at 189 cm^{-1} , 337 cm^{-1} , 492 cm^{-1} , 652 cm^{-1} , 697 cm^{-1} as seen in Table 4. Normally modes above 600 cm^{-1} correspond to the a distortion or vacancy sites in ferrites (Li *et al.*, 2017; Murugesan, 2013). Broadening of modes in Raman spectra is due to the strain developments and reduction in grain size (Murugesan *et al.*, 2015) in bulk crystalline ferrite. The mass difference between the three ions (Ni^{2+} , Fe^{3+} , Zn^{2+}) splits the mode in three different energy values. The lightest ion Ni^{2+} corresponds to around 697 cm^{-1} for $x=0.3$ to 0.5 the heaviest one i.e., Fe^{3+} corresponds to around 554 cm^{-1} and an intermediate mode of Zn^{2+} ions around 572 cm^{-1} , 569 cm^{-1} . The relative intensity and peak position can be explained considering the effects, resulting from introducing Zn ion and its increasing content.

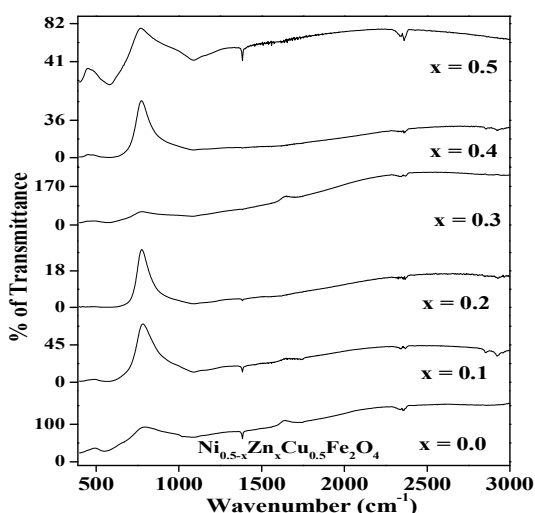
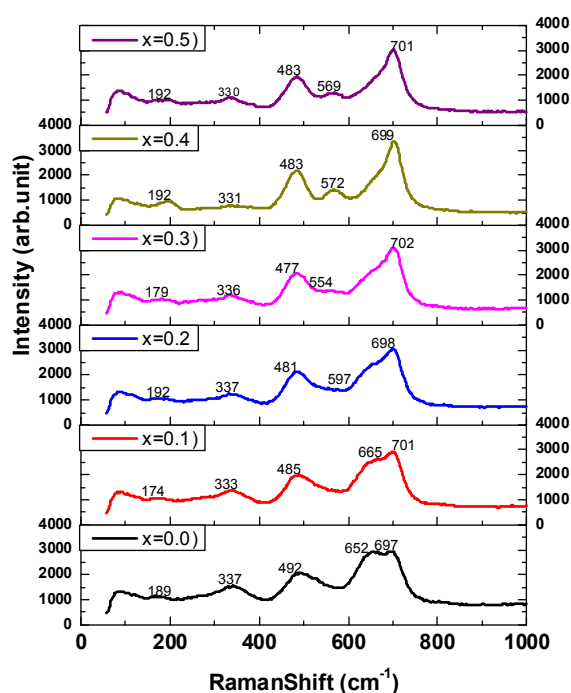
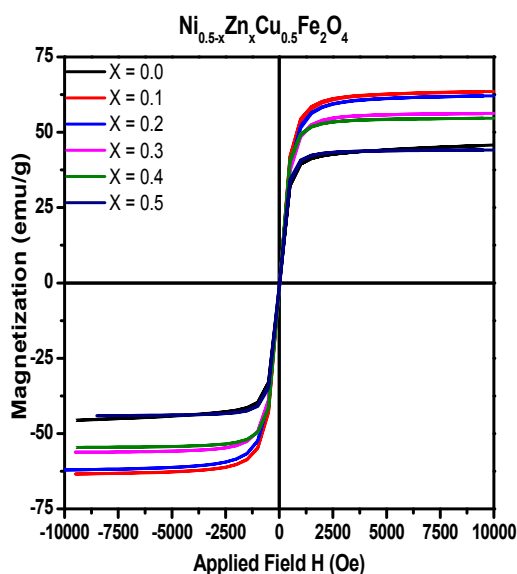
Figure 3. FTIR spectra of $\text{Ni}_{0.5-x}\text{Zn}_x\text{Cu}_{0.5}\text{Fe}_2\text{O}_4$ systemFigure 4. Raman spectra of $\text{Ni}_{0.5-x}\text{Zn}_x\text{Cu}_{0.5}\text{Fe}_2\text{O}_4$ systemFigure 5. Magnetic hysteresis loop of $\text{Ni}_{0.5-x}\text{Zn}_x\text{Cu}_{0.5}\text{Fe}_2\text{O}_4$ system

Table 2. Ionic radii and magnetic moments of the cations

Cations	Ionic radius (Å)	Magnetic moments (μB)
Fe^{3+}	0.6	5.92
Fe^{2+}	0.74	4.90
Ni^{2+}	0.69	2.84
Zn^{2+}	0.74	0.0
Cu^{2+}	0.72	1.73

Table 3. Centre frequencies of the bands of FTIR spectra of the sintered $\text{Ni}_{0.5-x}\text{Zn}_x\text{Cu}_{0.5}\text{Fe}_2\text{O}_4$ system

Concentration (X)	ν_1	ν_2
0.0	453.20	775.27
0.1	495.63	744.41
0.2	503.35	740.56
0.3	543.85	732.84
0.4	518.77	725.13
0.5	522.63	773.34

Table 4. Centre frequencies of the bands of Raman spectra of the sintered $\text{Ni}_{0.5-x}\text{Zn}_x\text{Cu}_{0.5}\text{Fe}_2\text{O}_4$ system

Concentration	Centre frequency cm^{-1}				
X	V1	V2	V3	V4	V5
0.0	189	337	492	652	697
0.1	174	333	485	665	701
0.2	192	337	489	597	698
0.3	179	336	477	554	702
0.4	192	331	483	572	699
0.5	192	330	483	569	701

Further the Raman frequencies depend on the Fe (Ni) -O and bond length. The intensity of the highest wavelength Raman mode (initially around 697cm^{-1}) decreases with increasing Zn contents the intensity of the Raman mode peaking around 702cm^{-1} increases proportionally. Thus the vacancy/ defect states formation is consistently observable in Raman as seen in IR spectra. Further the presence of absorption modes of respective sites namely octahedral and tetrahedral sites is confirming spinel formation.

Magnetic Study

Zinc substituted nickel, copper ferrite samples having the chemical formula $\text{Ni}_{0.5-x}\text{Zn}_x\text{Cu}_{0.5}\text{Fe}_2\text{O}_4$ (where $x=0.0,0.1,0.2,0.3,0.4,0.5$) are subjected magnetic study. The room temperature magnetisation curves of the sample are shown in Fig. 5. These show variation of magnetization, coercive field zinc content. Magnetic parameters, namely the specific magnetization (M_s), remnant magnetization (M_r) and coercive field (H_c) of the prepared fine particles $\text{Ni}_{0.5-x}\text{Zn}_x\text{Cu}_{0.5}\text{Fe}_2\text{O}_4$ are measured at room temperature in a maximum field of 10000 gauss. The values of magnetic parameters are given in Table 5. It is noticed that magnetic properties of the samples are strongly dependent on the zinc concentration. The saturation magnetization (M_s) for the sample (system) was found to increase from $x=0.1$ to 0.4. Here is an increase in from $x=0.1$ to 0.2 and for $x=0.5$ M_s is very low. It is observed that the saturation magnetisation decreases. The respective reduction in magnetisation can be due to a rearrangement of cations, a change in distribution of Ni^{2+} and Zn^{2+} on the two sites (Tarte, 1967). In the present study the parameters of primary importance saturation magnetisation, coercive field remanance magnetisation and M_r/M_s ratio. The shape of hysteresis loop render explanation for the nature of a magnetic domain and type of the magnetic material. According to the fairly well established consideration, the loops obtained for the $\text{Ni}_{0.5-x}\text{Zn}_x\text{Cu}_{0.5}\text{Fe}_2\text{O}_4$ quenched system Fig.5 of the present study are indicative of multi-domains (Chandrasekaran, 2004).

Table 5. Saturation magnetisation (Ms), remanent magnetisation (Mr), Mr/Ms ratio and coercive field (Hc) of sintered Ni_{0.5-x}Zn_xCu_{0.5}Fe₂O₄

Concentration X	Saturation magnetisation (Ms) emu/g	Remanent magnetisation (Mr) emu/g	Mr/Ms ratio	Coercive field (Hc) Oe
0.0	45.7615	2.0273	0.0443	0.9600
0.1	62.4325	1.9373	0.0305	0.8180
0.2	62.0934	1.9659	0.0316	3.7532
0.3	56.2351	1.2910	0.0229	6.6943
0.4	54.6398	1.3983	0.0255	6.68147
0.5	44.1236	1.2006	0.0272	10.0161

The values of coercive field varies between 0.82 Oe and 10.01 Oe, it is seen from the Table 5. That the coercive field is found to be fairly low and there is no much change with respect to concentration low value of coercive field is effected due to soft nature of the ferrite. It is found to be insensitive to concentration variation. The values of remanant ratio ranges from 0.0272 to 0.0443. Therefore it is understood that the ferrite prepared in the present study are multi domain cases (Li, 2017; Cullity, 2011). The saturation magnetisation (Ms) values ranges from 44emu/g to 62emu/g and. These values are in good agreement with the values reported by I. Neel (2013) and C. murugesan (Néel, 1952) for the similar types of ferrite. The present samples belong to cubic system of ferromagnetic spinel. In these systems the magnetic order is mainly due to an indirect exchange interaction mechanism occurring between the metal ions in the A and B sub lattices. The substitution of Zn²⁺ ions, which has a preferential A site occupancy results in the reduction of the exchange interaction between A and B sites. Hence magnetic properties of the particle can be varied by varying the degree of zinc substitution. Thus the changes in H_c and M_s Values are attributable to A-B and B-B exchange interactions. Which could be caused by Zn variation and na no size particle. However study using Mossbauer spectrometer would give clear information about the magnetic structure of the ferrite to understand in terms of Neel's two sub lattice models and canting spin on B site (Néel, 1952).

Conclusion

Ultra fine crystallites of Ni_{0.5-x}Zn_xCu_{0.5}Fe₂O₄ system of ferrites are prepared using solid state route along with post quenching in Nitrogen liquid bath followed by a wild grinding of the solid pellet. XRD reports the lattice shrinking for Zn substitution. FTIR and Raman measurements confirm spinel structure of the ferrites prepared and show additional bands indicating the defect states due to quenching. Magnetic studies explain the enhancement of magnetisation in terms of change in the exchange interaction as there is unusual distribution of ions in sites due to the quenching of ferrites sample. Thus quenching along with wild grinding of sample during synthesis leads to formation of ultra-fine crystallites which house amusing change of magnetic properties.

REFERENCES

- Chandrasekaran, G., Selvanandan, S., Manivanane, K. 2004. Electrical and FTIR Studies on Al Substituted Mn-Zn mixed ferrites. *Journal of Materials Science: Materials in Electronics* 1515-18.
- Choi, Y., Shim, H., Lee, J. 2001. Study on magnetic properties and structural analysis of Ni-Zn ferrite prepared through self-propagating high-temperature synthesis reaction by neutron diffractometry, *J. Alloys Compd.*, 326 56-60.
- Cullity, B.D., Graham, C.D. 2011. Introduction to magnetic materials, John Wiley & Sons.
- Cullity, B.D., Weymouth, J.W. 1957. Elements of X-ray Diffraction, *American Journal of Physics*, 25 394-395.
- Dias, A., Moreira, R. 1999. Chemical, mechanical and dielectric properties after sintering of hydrothermal nickel-zinc ferrites, *Mater. Lett.*, 39 69-76.
- Erdemi, H., Baykal, A. 2015. Dielectric properties of triethylene glycol-stabilized Mn 1-x Zn x Fe 2 O 4 nanoparticles, *Mater. Chem. Phys.*, 165 156-167.
- Gawas, S.G., Gawas, U.B., Verenkar, V.M.S., Kothawale, M.M., Pednekar, R. 2016. Structural and Magnetic Studies of Cu-Substituted Nanocrystalline Ni-Zn Ferrites Obtained Via Hexamine-Nitrate Combustion Route, *Journal of Superconductivity and Novel Magnetism*, 1-6.
- Goldman, A. 2006. Ferrites for Magnetic Recording, *Modern Ferrite Technology*, 353-373.
- Golkhatmi, F.M., Bahramian, B., Mamarabadi, M. 2017. Application of surface modified nano ferrite nickel in catalytic reaction (epoxidation of alkenes) and investigation on its antibacterial and antifungal activities, *Materials Science and Engineering: C*, 78 1-11.
- Hartmann-Boutron, F., Imbert, P. 1968. Mössbauer Study of the Electronic and Magnetic Properties of Fe²⁺ Ions in Some Spinel-Type Compounds, *J. Appl. Phys.*, 39 775-785.
- Jacobo, S., Fano, W., Razzitte, A. 2002. The effect of rare earth substitution on the magnetic properties of Ni 0.5 Zn 0.5 M x Fe 2-x O 4 (M: rare earth), *Physica B: Condensed Matter*, 320 261-263.
- Journal of material sciences: materials in Electronics* 15(2004)15-1
- Kumar, K.V., Ravinder, D. 2002. Electrical conductivity of Ni-Zn-Gd ferrites, *Mater. Lett.*, 52 166-168.
- Kwon, J., Kim, J.H., Kang, S.H., Choi, C.J., Rajesh, J.A., Ahn, K.S. 2017. Facile hydrothermal synthesis of cubic spinel AB₂O₄ type MnFe₂O₄ nanocrystallites and their electrochemical performance, *Appl. Surf. Sci.*, 413 83-91.
- Li, L.Z., Zhong, X.X., Wang, R., Tu, X.Q. 2017. Structural, magnetic and electrical properties of Zr-substituted NiZnCo ferrite nanopowders, *J. Magn. Mater.*, 435 58-63.
- Li, Y.X., Li, J., Li, Q., Yu, G.L., Zhang, H.W. 2017. Structure and magnetic properties of NiCuZn ferrite materials with La doping, *Rare Metals*, 36 202-204.
- Modi, K., Tanna, P., Laghate, S., Joshi, H. 2000. The effect of Zn²⁺ substitution on some structural properties of CuFeCrO₄ system, *J. Mater. Sci. Lett.*, 19 1111-1113.
- Mohan, G.R., Ravinder, D., Reddy, A.R., Boyanov, B. 1999. Dielectric properties of polycrystalline mixed nickel-zinc ferrites, *Mater. Lett.*, 40 39-45.
- Murugesan, C., Chandrasekaran, G. 2015. Impact of Gd³⁺ substitution on the structural, magnetic and electrical

- properties of cobalt ferrite nanoparticles, RSC Advances, 5 73714-73725.
- Murugesan, C., MDgazzali, P.M., Chandrasekaran, G. 2013. Influence of oxidizer to fuel ratio on structural and magnetic properties of Mn–Zn ferrite nanoparticles, *Journal of Materials Science: Materials in Electronics*, 24 3136-3141.
- Murugesan, C., Perumal, M., Chandrasekaran, G. 2014. Structural, dielectric and magnetic properties of cobalt ferrite prepared using auto combustion and ceramic route, *Physica B: Condensed Matter*, 448 53-56.
- Naghib zadeh, H., Oder, G., Hesse, J., Reimann, T., Töpfer, J., Rabe, T. 2016. Effect of oxygen partial pressure on co-firing behavior and magnetic properties of LTCC modules with integrated NiCuZn ferrite layers, *J. Electroceram.*, 37 100-109.
- Nanoti, V., Prakash, C., Kulkarni, D. 1995. Magnetic behaviour of Cr-substituted Zn-Cu ferrites, *Mater. Lett.*, 24 167-169.
- Néel, L. 1952. Antiferromagnetism and ferrimagnetism, *Proceedings of the Physical Society. Section A*, 65 869.
- Özgür, Ü., Alivov, Y., Morkoç, H. 2009. Microwave ferrites, part 1: fundamental properties, *Journal of Materials Science: Materials in Electronics*, 20 789-834.
- Ravinder, D., Kumar, K.V., Boyanov, B. 1999. Elastic behaviour of Cu–Zn ferrites, *Mater. Lett.*, 38 22-27.
- Ravinder, D., Mohan, G.R. 2000. Thermoelectric power studies of zinc-substituted nickel ferrites, *Mater. Lett.*, 44 139-143.
- Rezlescu, N., Rezlescu, E. 1993. The influence of Fe substitutions by R ions in a Ni_xZn_{1-x}Ferrite, *Solid State Commun.*, 88 139-141.
- Rezlescu, N., Rezlescu, E., Pasnicu, C., Craus, M. 1994. Effects of the rare-earth ions on some properties of a nickel-zinc ferrite, *J. Phys.: Condens. Matter*, 6 5707.
- Sileo, E.E., Rotelo, R., Jacobo, S.E. 2002. Nickel zinc ferrites prepared by the citrate precursor method, *Physica B: Condensed Matter*, 320 257-260.
- Smit, J., Wijn, H.P.J. 1959. Ferrites.
- Srivastava, C., Shringi, S., Patni, M., Joglekar, S. 1984. Influence of the presence of Fe²⁺ ion in nickel-zinc ferrite, *Bull. Mater. Sci.*, 6 7-12.
- Stewart, S., Multigner, M., Marco, J., Berry, F., Hernando, A., Gonzalez, J. 2004. Thermal dependence of the magnetization of antiferromagnetic copper (II) oxide nanoparticles, *Solid State Commun.*, 130 247-251.
- Tarte, P. Infra-red spectra of inorganic aluminates and characteristic vibrational frequencies of AlO₄ tetrahedra and AlO₆ octahedra. *Spectrochimica Acta*, 1967, vol.23A, PP. 2127-2143.
- Tatarchuk, T., Bououdina, M., Macyk, W., Shyichuk, O., Paliychuk, N., Yaremiy, I., Al-Najar, B., Pacia, M. 2017. Structural, Optical, and Magnetic Properties of Zn-Doped CoFe₂O₄ Nanoparticles, *Nanoscale Research Letters*, 12 141.
- Verma, A., Goel, T., Mendiratta, R., Alam, M. 1999. Dielectric properties of NiZn ferrites prepared by the citrate precursor method, *Materials Science and Engineering: B*, 60 156-162.
- Viswanathan, B., Murthy, V. 1990. Ferrite materials: science and technology, Springer Verlag.
- Waldron, R. 1955. Infrared spectra of ferrites, *Physical review*, 99 1727.
- Yue, Z., Li, L., Zhou, J., Zhang, H., Gui, Z. 1999. Preparation and characterization of NiCuZn ferrite nanocrystalline powders by auto-combustion of nitrate–citrate gels, *Materials Science and Engineering: B*, 64 68-72.
